

# Investigation of a 3-D Undersea Positioning System Using Electromagnetic Waves

Ryosuke Kato<sup>1</sup>, Member, IEEE, Masaharu Takahashi, Senior Member, IEEE, Nozomu Ishii<sup>2</sup>, Member, IEEE, Qiang Chen<sup>3</sup>, Senior Member, IEEE, and Hiroshi Yoshida, Member, IEEE

**Abstract**—When divers rescue people from accidents at sea, they are in danger because of obstacles floating in the sea. If divers can confirm their own position, their activities will become much safer. In this study, assuming that we specify the positions of the divers performing rescue operations, to support their work, we investigate an undersea positioning technology using electromagnetic waves with low frequencies, i.e., 10 kHz. In previous studies, an ultra-long wave of 10 kHz was theoretically attenuated at 3.5 dB/m. In addition, a simulation of position estimation in the vertical section of the sea was reported. In this study, we indicate the superiority of using receiving signal strength (RSS) to the phase difference between a transmitted and received signal. We also investigate an algorithm for position estimation wherein the antenna characteristics and two propagating rays of electromagnetic waves at sea are considered. Finally, we estimate the position of the transmitting antenna at depths of 1 to 8 m using our algorithm.

**Index Terms**—Antenna, lateral wave, receiving signal strength (RSS), undersea positioning system.

## I. INTRODUCTION

IN RECENT years, many technologies have been developed to support the generation of new ocean businesses [1]–[3]. To date, acoustic waves have been commonly utilized for undersea wireless communications. This is because the attenuation of acoustic waves is smaller than that of electromagnetic waves and light waves, and it is suitable for remote communication at sea [4], [5]. However, it propagates at 1.5 km/s in the ocean, which is considerably slow, approximately one-fiftieth as fast as that of electromagnetic waves. Furthermore, the effect of the temperature and salinity concentration of seawater should be considered. According

to [6], the diffraction depending on the depth of the sea may also be of concern. Regarding light waves, the scattering attenuation with the muddiness of the seawater is large. Pompili and Akyildiz [2] proposed that light-wave telecommunication in seawater is unsuitable owing to the instability and capability of communication. Because electromagnetic waves have a large attenuation, it is considered that undersea communication with electromagnetic waves is very difficult [7]. However, the reflection and diffraction of electromagnetic waves can be ignored because of their large attenuation. Thus, we wish to consider using electromagnetic waves in the sea, especially in shallow seas.

According to [8]–[10], studies of telecommunication employing frequencies of lower-than-MHz bands were often conducted through the 1970s. Since the attenuation of undersea electromagnetic waves was considerably large, no further studies employing electromagnetic waves in the sea were made at that time. However, according to [11]–[13], there is an increasing trend to determine methods of employing electromagnetic waves for telecommunication in the sea. This trend is because of the propagation experiments of electromagnetic waves in seawater conducted in England in the 1990s [14]. On the other hand, instabilities were of concern in the cases of acoustic waves and light waves for telecommunication. Because acoustic waves in the sea have an attenuation of almost zero, all reflections and diffractions are received in the shallow sea and around the seabed. In such a place, it is difficult to distinguish direct waves from reflections and diffractions. Authors [15]–[19] showed that some discussions and considerations for undersea telecommunication technologies were resumed, compared to the 1960s, with a dramatic improvement in wireless telecommunication, digital communication technologies, and computational electromagnetics. These approaches utilize the advantages of minimal reflection owing to the large attenuation of electromagnetic waves in the sea.

We consider the development of supporting technologies for water rescues as a way of using electromagnetic waves in seawater. Several accidents occur in water worldwide. According to the study mentioned in [20], the number of accidents is high, and the number of dead and missing people is also high. Accidents in the water are predominantly because of natural disasters and sinking accidents involving ships. However, the view of divers in the sea during the rescue is sometimes obscured, and there are various obstacles floating

Manuscript received March 27, 2020; revised December 8, 2020; accepted December 13, 2020. Date of publication January 8, 2021; date of current version August 4, 2021. This work was supported by the Chiba University SEEDS Fund (Chiba University Open Recruitment for International Exchange Program). (Corresponding author: Ryosuke Kato.)

Ryosuke Kato is with the Graduate School of Science and Technology, Chiba University, Chiba 263-8522, Japan (e-mail: affa2167@chiba-u.jp).

Masaharu Takahashi is with the Center for Frontier Medical Engineering, Chiba University, Chiba 263-8522, Japan (e-mail: masa@ieee.org).

Nozomu Ishii is with the Faculty of Engineering, Niigata University, Niigata 950-2181, Japan (e-mail: nishii@eng.niigata-u.ac.jp).

Qiang Chen is with the Department of Communications Engineering, Tohoku University, Sendai 980-8579, Japan (e-mail: chenq@ecei.tohoku.ac.jp).

Hiroshi Yoshida is with the Department of Engineering for Geo-Marine Sciences, Japan Agency for Marine-Earth Science and Technology, Yokosuka 237-0061, Japan (e-mail: yoshidah@jamstec.go.jp).

Color versions of one or more figures in this article are available at <https://doi.org/10.1109/TAP.2020.3048584>.

Digital Object Identifier 10.1109/TAP.2020.3048584

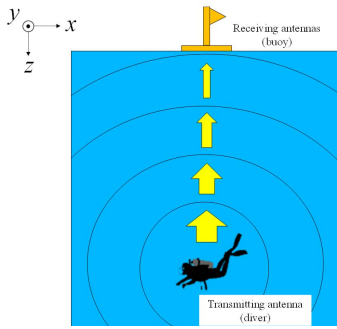


Fig. 1. Image of undersea position estimation.

in the water. Therefore, consideration of the safety of the divers during the rescue is required. Rescue activities will become much safer if divers know their own current positions during the rescue. Therefore, it is essential to establish an undersea positioning system based on wireless communication technologies.

Since divers are constantly moving during the rescue, the system must possess real-time positioning. However, the environment in which they work has various factors to be considered for undersea positioning systems. Thus, a simple algorithm and processing with little calculation are needed.

In this study, we consider an underwater positioning system that utilizes the frequency in kHz bands to establish technologies that divers can employ easily in sea accidents. As a positioning system currently used in the ocean, the global positioning system (GPS) is widely used. For GPS, receivers on the ground receive electromagnetic waves transmitted by four architected satellites. Using the information, GPS specifies the position and corrects the time employed. However, we cannot use GPS in places where electromagnetic waves cannot reach, such as inside caves or the sea. In such places, there are positioning technologies that match patterns to data collected in advance and utilize the attenuation of electric power through propagation [21].

In the positioning technique using the attenuation, we conduct positioning by estimating the propagation distances using the received powers, drawing the sphere with the radius of the estimated distance whose center is each receiver, and calculating the cross point of the spheres.

The undersea environment is where satellite signals are unreachable, making it difficult to collect data in advance. Therefore, we consider a positioning system employing the difference in the attenuation of power in the seawater or the phase difference between the transmitted and received signals. Fig. 1 shows a simulation model of the positioning in the sea.

A diver is carrying an oxygen tank with a transmitting antenna on his/her back. A receiver is installed on a buoy. We calculate the position using the received powers or phases of transmitting signals. In this study, we investigate a 3-D undersea positioning system employing electromagnetic waves for easy utilization in accidents at sea. Although electromagnetic waves have not been employed owing to their large attenuation, it is expected that the investigation carried out in this study will expand the employment of electromagnetic waves in the sea.

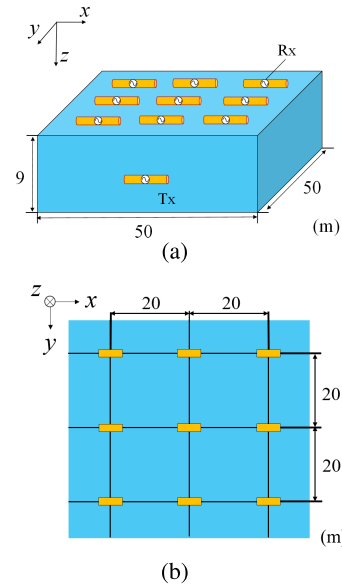


Fig. 2. Sea model for the undersea antenna position estimation. (a) Overview. (b) Overhead view.

In the preceding study, we developed an algorithm for an undersea positioning system [22]. In this algorithm, the correction of RSS is circulated three times. In this article, we propose a new algorithm that is not circulated and more accurate by changing how to select the first estimated position.

Section II presents the simulation model for the investigation of undersea position technology and operating frequency.

In Section III, we explain the parameter utilized for the positioning system and why we chose that parameter. In addition, we explain how to calculate the antenna's distance from that parameter.

Section IV shows the factors that affect undersea positioning technologies and explain how to process these factors.

Section V explains how to correct the received signals by employing angles between transmitting and receiving antennas to make the positioning system more accurate.

In Section VI, we present the results of an undersea antenna positioning simulation based on Sections III and IV.

Finally, Section VII presents the conclusion.

## II. ASSUMED POSITION ESTIMATION SYSTEM

For the position estimation in the sea, we assume an ideal environment, which is shallow and has a sea surface with no waves. We employed one-axis dipole antennas for our simulations as a basic study for a positioning system of undersea antennas. The simulation model is shown in Fig. 2.

The model has a free space with a height of 2 m and seawater with a depth of 9 m ( $\epsilon_r = 80$ ,  $\sigma = 4.0$  S/m). Nine 2-m receiving antennas (Rxs) are dipole antennas installed horizontally on the sea surface at intervals of 20 m. We assume that all Rxs are fixed on something like a raft, and the distance between each Rx is constant. A 0.7 m transmitting antenna (Tx) is a dipole antenna installed at any point in the sea. The electric constants in the sea are based on [23]. This system requires a spatial resolution of 2 m, which is the size of a diver's outstretched arm, and a positioning range

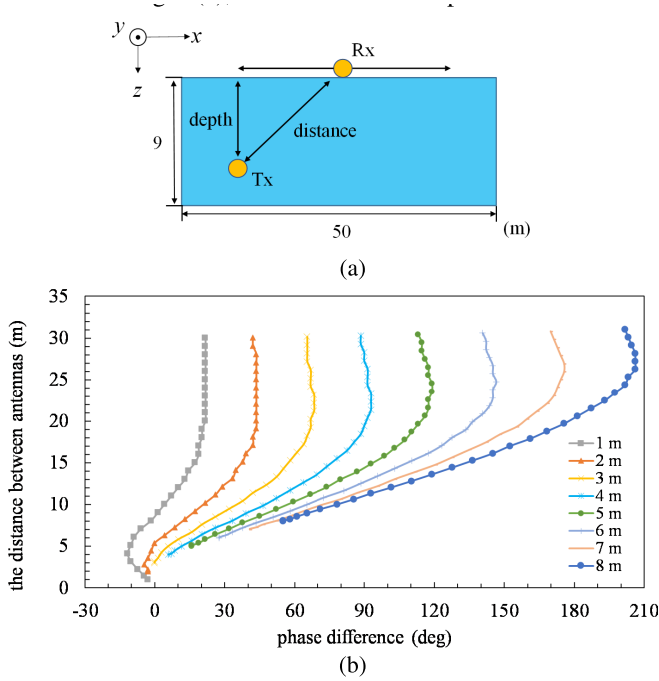


Fig. 3. Relation between the phase differences and the antenna distances at each depth from 1 to 8 m. (a) Model for analysis. (b) Result of the analyses.

of 30 m. In [24], the distances that the electromagnetic waves attenuate 100 dB in the sea at each frequency have been investigated. According to [24], ultra-long waves of 10 kHz attenuate at 3.5 dB/m theoretically. Considering the dynamic range of measuring instruments (−100 dB), a 10 kHz wave can propagate up to 30 m. In addition, we can distinguish the distance at 1 m intervals with 10 kHz waves. Therefore, we utilized 10 kHz waves for the positioning simulation within a sphere, with a radius of 30 m.

In this simulation, we employed the finite-difference time-domain (FDTD) method. All cells are 0.1 m × 0.1 m × 0.1 m, and the time step is 1.920 × 10<sup>−10</sup> s, which satisfies the Courant limit. This calculation is iterated 2 million times. As a boundary condition, 20 layers of PML were deployed. The Tx is divided into seven cells, and the Rx is divided into 21 cells. Moreover, we feed a 1 V sinusoidal wave into a Tx constantly.

### III. CALCULATING DISTANCE OF ANTENNAS

In this section, we explain why we selected the RSS rather than the phase difference when calculating the distance between antennas, and how to calculate the distance via RSS.

In Fig. 3, we show the model for analyzing the relationship between the phase difference and the antenna distance numerically, as well as the result of the analysis. We analyzed the phase of the electromagnetic signal at each position of Tx and Rx shown in Fig. 3(a), and calculated the phase differences.

The parameters were calculated using two dipole antennas, which were deployed in parallel as shown in Fig. 3(a). Fig. 3(b) shows the phase distribution regarding the distance between the antennas at each depth per 1 m. In Fig. 3, the phase difference shows constant values at more than a certain distance. This is because of the lateral wave. First,

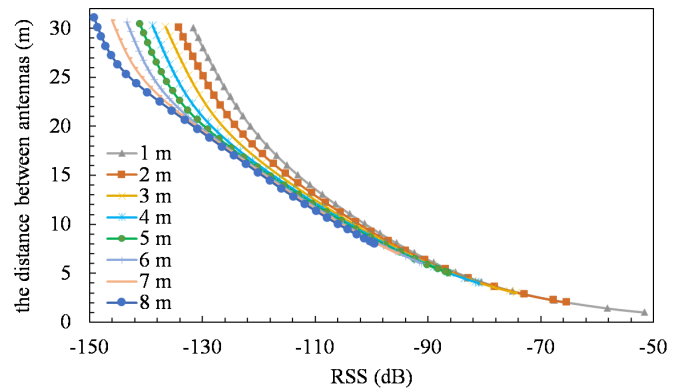


Fig. 4. Relation between RSS and the antenna distances at each depth from 1 to 8 m.

electromagnetic waves in the sea propagate to the sea surface perpendicularly. This is because waves only propagate almost vertically according to the boundary conditions. Lateral waves propagate from the point at the sea surface just above the wave source. According to [25]–[29], lateral waves exist. A lateral wave has a long wavelength in the air; thus, its phase is nearly the same while it is propagating through the air. In Fig. 3, the intensity of the direct waves in the sea remains strong at up to 15 m, which causes phase changes. However, at longer distances, the propagation in the sea is greatly attenuated, so that only a lateral wave component exists and no phase change. Therefore, calculating the antenna distance over 15 m with the phase difference is difficult, which is not satisfied with the requirement of a positioning range of 30 m.

Subsequently, we show the RSS regarding the distance between the antennas at each depth per 1 m in Fig. 4.

The parameters in Fig. 4 were calculated, as shown in Fig. 3(a). RSS is a logarithm of the ratio of the received power to the input power

$$\text{RSS (dB)} = 10 \log_{10} \frac{\text{Received power (W)}}{\text{Input power (W)}}. \quad (1)$$

We calculated the RSS as (1). Here, we focus only on the relative attenuation of the RSS signal. The 10 kHz wavelength is considerably long. Hence, considering the analysis of the small dipole antenna, the antenna matching is not aligned. By employing an underwater antenna, the absolute intensity of the RSS is confirmed to be within the dynamic range of the instrument [12], [30]. RSS is distinguishable even when the antenna distance is over 30 m in Fig. 4, considering only the difference in the attenuation. Therefore, we decided to employ RSS in this study’s undersea positioning simulation

$$r = \sum_{k=1}^5 C_{k,z} p^k. \quad (2)$$

The polynomial approximation of (2) was used to calculate the antenna distances from the RSS, where  $r$  is the antenna distance and  $p$  represents the RSS. Equation (2) is the approximate expression of the relation in Fig. 4, and  $C_{k,z}$  was employed to calculate the antenna distances based on the RSS. Variable  $z$ , the depth at which Tx exists, is an integer value from 1 to 8. When Tx is at a non-integer depth, we estimate

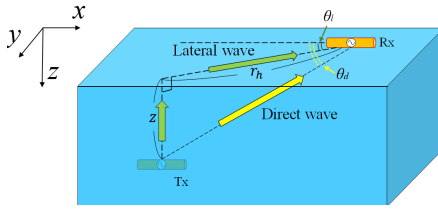


Fig. 5. Two propagating rays of an undersea electromagnetic wave.

its position using the nearest integer depth. In the case of a depth of 4.5 m of Tx, we calculate two distances using  $z$  of 4 and 5 and treat the average of the two calculated values as  $r$ .

#### IV. FACTORS AFFECTING UNDERSEA POSITIONING SYSTEM

In this section, we consider the factors that affect undersea positioning systems. There are two main factors that affect undersea positioning systems.

One factor is the lateral wave. The electromagnetic wave propagates through two rays in the sea. Fig. 5 shows an image of the propagation of each wave in the sea.

In Fig. 5, Tx is located arbitrarily. In this diagram, Tx is at a different Y coordinate as compared to Rx. One wave propagates through the shortest distance between antennas, which we refer to as the direct wave. The other is the lateral wave shown in Section III. In Fig. 5,  $\theta_d$  shows the incident angle from a direct wave, which is the angle between the axis of Rx and the propagating line of a direct wave. Also,  $\theta_l$  indicates the incident angle from a lateral wave, which is made between the axis of Rx and the extended line of the green arrow on the sea surface, as shown in Fig. 5. Both direct and lateral waves are received in Rx. While direct waves propagate in the sea with large attenuation, lateral waves pass through the sea only when propagating vertically. As indicated in Section III, direct waves are superior to lateral waves in the field of close distances between antennas. However, the attenuation of direct waves increases with antenna distance, and only lateral wave components remain. In the field of antenna distances over 15 m in Figs. 3 and 4, the phase differences are extremely small, but the RSS changes at a constant rate according to the antenna distance. Thus, the antenna distances can be identified from only the differences in the RSS within the target positioning area.

The other factor is the angular characteristics. The differences in the RSS at each angle are shown in Fig. 6.

A Tx is installed at a depth of 4 m, and an Rx is installed on the sea surface. These antennas are both dipole antennas deployed in parallel at a distance of 20 m. Since the characteristics of dipole antennas are not isotropic, there are some differences in the RSS at each angle. Considering the 10 kHz wavelength, the target area for our system is in an extremely near field. In this area, the radiation of the axis direction of a dipole antenna is not null. In Fig. 6, the RSS differences are at most 10 dB.

#### V. ANGLE CORRECTION

In Section IV, we confirmed that lateral waves and the characteristics of antennas can affect undersea positioning

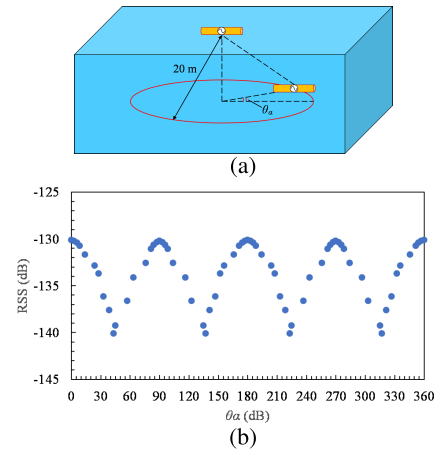


Fig. 6. Characteristic of RSS at each angle. (a) Model for analysis. (b) Difference of RSS at each angle.

systems via RSS. Therefore, the received powers must be corrected using  $\theta_d$  and  $\theta_l$ . In this section, we show how to correct the received powers by employing  $\theta_d$  and  $\theta_l$ . The following equation is the equation for angle correction:

$$P_{corrected} = P + \Delta P. \quad (3)$$

The variable  $P$  represents RSS, and  $\Delta P$  is a value to correct. The RSS corrected by angle correction is  $P_{corrected}$ .

#### A. Theoretical Received Signals From a Direct and Lateral Wave

We considered an algorithm for estimating the position of an undersea Tx. In this algorithm, we correct the received signals by employing theoretical values of the direct and lateral waves based on the theoretical equations of an electric field. In this section, we show the equation of the electric field strength of each wave derived from Maxwell's equations, and then we calculate the theoretical value of each wave from those equations. Here, a 10 kHz wavelength is approximately 16 m in the sea. Since the length of a Tx is 0.7 m, we treat the antennas employed as infinitesimal current elements.

The Tx is installed in the parallel direction of Rx, as shown in Fig. 5. Therefore, the electric field  $E_x$  in Fig. 5 is predominant for the received power. Although the equations in the two-layered media with seawater and air were deduced in [31] and [32], these have an assumption of  $r_h \gg z$ . Therefore, we derived equations suitable for this system. The electric field  $E_x$  can be expressed as (4) using the equation of radiation from an infinitesimal current element [33]. The permittivity of the sea is indicated as  $\epsilon$ , and the distance between Tx and Rx is represented using  $r$ :

$$\begin{aligned} E_x &= E_r \cos \theta_d - E_\theta \sin \theta_d \\ &= \frac{I l e^{-jkr}}{j4\pi\omega\epsilon} \left\{ 2 \left( \frac{1}{r^3} + \frac{jk}{r^2} \right) \cos^2 \theta_d \right. \\ &\quad \left. - \left( \frac{1}{r^3} + \frac{jk}{r^2} - \frac{k^2}{r} \right) \sin^2 \theta_d \right\}. \quad (4) \end{aligned}$$

Because the dielectric loss tangent  $\tan \delta$  is much larger than 1, the complex permittivity  $\epsilon$ , wave constant  $k$ , and

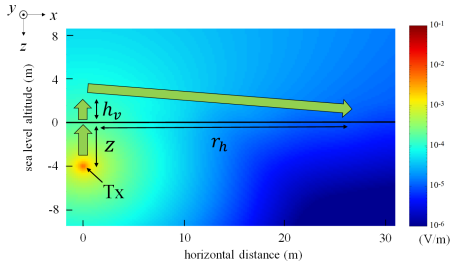


Fig. 7. Approximating propagating way of lateral wave.

attenuation constant  $\alpha$  are approximated in the following:

$$\begin{aligned}\epsilon &= \epsilon + \frac{\sigma}{j\omega} \simeq \frac{\sigma}{j\omega} \\ k &= \sqrt{\omega^2 \epsilon \mu - j\omega \mu \sigma} \simeq \alpha(1 - j) \\ \alpha &\simeq \beta \simeq \sqrt{\frac{\omega \mu \sigma}{2}}.\end{aligned}\quad (5)$$

The variable  $\sigma$  is the electric conductivity, and  $\mu$  is the magnetic permeability. The electric power is directly proportional to the square of the electric field strength. Thus, the absolute value of  $E_x$  in the sea is approximated by the following:

$$\begin{aligned}|E_x| &\simeq \frac{I l e^{-\alpha r}}{4\pi \sigma r^3} \\ &\times \sqrt{(3 \cos^2 \theta_d - 1)^2 (1 + \alpha r)^2 + \alpha^2 r^2 \{2 - (3 + 2\alpha r) \sin^2 \theta_d\}^2}.\end{aligned}\quad (6)$$

Since we assume that Rx is floating on the sea surface, the electric power from a direct wave is calculated using (6). On the other hand, a lateral wave moves vertically through the sea and propagates to an Rx horizontally in the air. This indicates that the power of a lateral wave can be calculated using (6) while propagating in the sea, and the re-radiation of the lateral wave arriving at the sea surface spreads concentrically in the air. If we define the electric field just above Tx on the sea surface as the vector  $\mathbf{E}_{surface}$ , then the electric field of the re-radiation in the air is indicated as (7) because  $\sigma$  is zero and  $\beta r_h$  is almost zero in the analytical model

$$|E_l| \simeq \frac{\int_S \sigma \mathbf{E}_{surface} \cdot \mathbf{n} dS}{4\pi \omega \epsilon_0 \left( h_v + \sqrt{h_v^2 + r_h^2} \right)^3} |3 \cos^2 \theta_l - 1|. \quad (7)$$

The vector  $\mathbf{E}_l$  shows a theoretical formula of the lateral wave, and  $\sigma \mathbf{E}_{surface}$  is the inductive electric current generated by the electric field of the electromagnetic wave propagating just above. In addition,  $S$  is the sectional area of the inductive electric current,  $\epsilon_0$  is the permittivity of the air, and  $r_h$  is the horizontal distance from the above point of Tx to Rx. Here, we consider the distance  $h_v$ . Fig. 7 shows the distribution of the electric field strength from Tx at a depth of 4 m and an approximating propagating behavior of the lateral wave.

The lateral wave factually propagated slightly vertically in the air, indicated as  $h_v$  in Fig. 7. Since the wavelength extends largely when the electromagnetic wave permeates the sea surface, we need to consider  $h_v$ .

Therefore, (7) is represented as the following:

$$|E_l| \simeq \frac{\int_S I l e^{-\alpha z} \sqrt{(1 + \alpha z)^2 + \alpha^2 z^2 (1 + 2\alpha z)^2} dS}{16\pi^2 \omega \epsilon_0 z^3 \left( h_v + \sqrt{h_v^2 + r_h^2} \right)^3} \times |3 \cos^2 \theta_l - 1|. \quad (8)$$

Variable  $z$  represents the depth of the Tx. Equation (8) indicates the absolute value of the lateral wave.

Summarizing the above, (6) represents the electric field strength from the direct wave, and (8) shows that of the lateral wave. The following equation is the relation between the received electric power and the electric field.  $K_d$  and  $K_l$  are the constants of proportionality including the antenna effective area and the gain of the antenna

$$P_{d(or)l} \text{theo} = K_{d(or)l} |E_{d(or)l}|^2. \quad (9)$$

### B. First Selection of Estimated Tx's Area for RSS Correction

To correct the RSS accurately, it is necessary to calculate accurate theoretical values. Therefore, it is necessary to estimate the position of the Tx as close as possible before correcting the RSS. The estimated position of a Tx using the uncorrected RSS is distant from the actual position, affected by the factors shown in Section IV. For that, we limit the area where Tx exists by employing the two-dimensional distributions of RSS for the accurate correction of RSS. In this section, we explain how to limit the area of the Tx. First, we choose the four Rx's whose RSSs are the largest. The RSSs tend to be larger as the distances between the antennas decrease. Therefore, a Tx is expected to be the area surrounded by these antennas. Here, we show the distributions of the difference in dB of the largest RSS and the smallest one in four Rx's surrounded by the four top-left Rx's in Fig. 2.  $\Delta \text{RSS}$  is shown in the following:

$$\Delta \text{RSS}(\text{dB}) = \text{RSS}(\text{max}) - \text{RSS}(\text{min}). \quad (10)$$

For example, we assume that the top-left four Rx's shown in Fig. 2(b) have the largest power from first to fourth. In Fig. 8, the area turns redder as the difference in RSS is smaller. By contrast, the area turns greener as the difference increases. These differences have characteristic distributions, which are almost the same at any depth, and any four Rx's are chosen. The differences in RSS are small around the center and large near each Rx. From this tendency, we can estimate the position of the Tx. Here, we assume that the top-left antenna has the largest RSS followed by the bottom-left, top-right, and bottom-right antennas, as shown in Fig. 2(b). Since the antenna distance increases as the RSS increases, the position of Tx may be in the red line shown in Fig. 9. Moreover, when the RSS of the bottom-left antenna is larger than that of the top-right antenna, the position of Tx can be within the blue triangle line. In addition, if  $\Delta \text{RSS}$  is approximately 30 dB, then the position of Tx is estimated within the purple square. We correct the RSS assuming that the Tx is in this purple area.

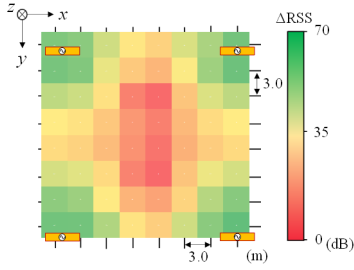


Fig. 8. Difference between the smallest and largest RSS.

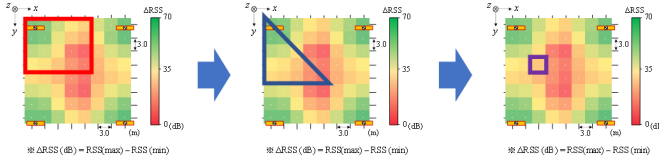


Fig. 9. Flow of deciding the first estimated position.

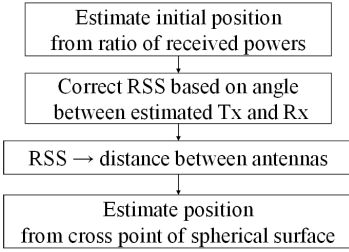


Fig. 10. Flow of the algorithm with the angle correction.

### C. Flow of Algorithm With Angle Correction

The algorithm for correcting the RSS based on each expected position of a Tx is shown in Fig. 10.

The estimation of the first position is shown in Section V (B). We conduct the correction of RSS employing  $\theta_d$  and  $\theta_l$  from the second step in the flow. First, we calculate the electric power of each wave based on the ratio of the theoretical electric power from each wave. Each power is calculated using the following:

$$P_d = \frac{P_{d,theo}}{P_{d,theo} + P_{l,theo}} P \quad (11)$$

$$P_l = \frac{P_{l,theo}}{P_{d,theo} + P_{l,theo}} P. \quad (12)$$

The variables  $P$ ,  $P_d$ , and  $P_l$  are the simulated values of the received electric power, direct waves, and lateral waves, respectively.  $P_{theo}$  are the theoretical values of the received electric power. In factual situations, it is assumed that electric characteristics are slightly different from those of the ideal model. These factors affect the direct and lateral waves as the coefficient of the electric field of each wave. Therefore, the received electric power based on the ratio, as shown in (11) and (12), should be more accurate than the theoretical values. In our algorithm, we calculate the distance between Rx and Tx using (2). However, (2) is deducted in the case of  $\theta_l = 90^\circ$ . Therefore, we adjusted the corrected powers to calculate the accurate distance. Finally, we summarize the corrected received powers again.

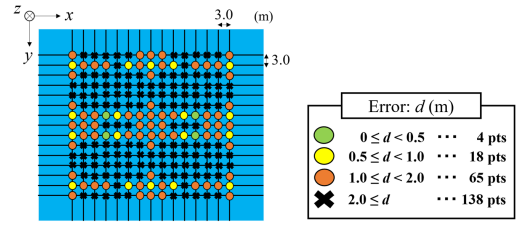


Fig. 11. Result without angle correction at depth 4 m.

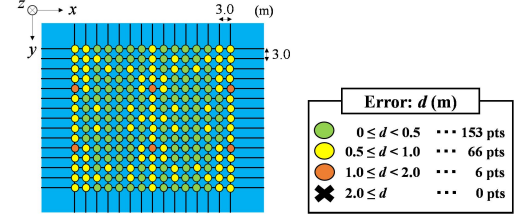


Fig. 12. Result of the position estimation at depth 4 m.

## VI. POSITION ESTIMATION RESULT

In this study, we simulated the position estimation of a Tx that exists at a depth of 1–8 m in the sea, based on the contents dictated here. In this section, we present the results of the positioning simulation. In addition, according to these results, we indicate the investigation to improve the accuracy for estimating the undersea Tx's position.

### A. Target Error of Position Estimation

As the target of the position estimation, we describe the target error against the factual position of a Tx. We evaluated the estimation accuracy based on the distance between the factual and estimated positions. Since we are considering the real-time estimation of the position of a diver in the sea in this study, we establish a maximum of 2.0 m as the target error, considering an adult male expanding his/her arms and legs.

### B. Position Estimation Result Without Angle Correction

First, we show the result of the position estimation in the case where the RSS is not corrected. Fig. 11 shows the result at a depth of 4 m.

The rate within the target error was 38.7%. Although the accuracy of the position estimation just beneath the Rx is comparably high, the estimation accuracy is very low.

### C. Position Estimation Result With Angle Correction

We show the position estimation result of Tx's at a depth of 4 m based on the algorithm with angle correction in Fig. 12. We achieved a target error within 2.0 m at all 225 points. Almost all errors are within 1.0 m, and 87% are within an error of 0.5 m.

We also indicate the results at depths of 1–8 m as the error frequency rates in Fig. 13.

As shown in Fig. 13, we achieved the target error at all integer depths from 1 to 8 m. The horizontal axis shows the error range; for example, the frequency of errors at 0.0–0.2 m of 1 m depth becomes 38%. Overall, most errors are achieved

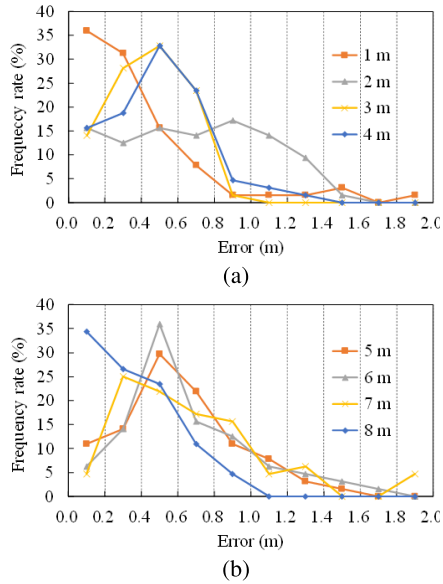


Fig. 13. (a) Error frequency rates at depths of 1–4 m. (b) Error frequency rates at depths of 5–8 m.

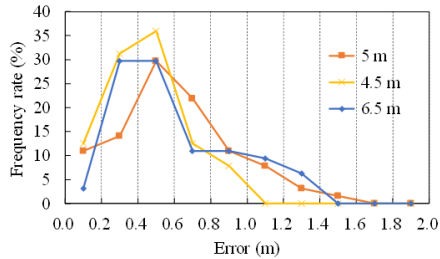


Fig. 14. Error frequency rates at depth 5, 4.5, and 6.5 m.

within 1.0 m. In particular, the errors at depths of 3 and 8 m are considerably small. Since we aim to specify the diver's position during the rescue, an error of 1.0 m is considerably accurate. Therefore, we can estimate Tx's positions with good accuracy at any integer depth. Furthermore, we show the results at noninteger depths of 4.5 and 6.5 m in Fig. 14. As a reference, the result at a depth of 5 m is also shown. We also achieved a target error within 2.0 m at these noninteger depths.

Therefore, the algorithm proposed in this article is useful.

## VII. CONCLUSION

We investigated the establishment of a position-estimating system for undersea antennas using electromagnetic waves, assuming that we employ the system for water accidents. In this process, we confirmed the superiority of RSS to phase difference in the case of position estimation in the sea. As a result, we achieved a target error within 2.0 m at all 225 points at depths of 1–8 m with our proposed algorithm. This algorithm has a single flow and is concise. From this investigation, we found that our proposed algorithm is worth using.

As a subject in the future, we need to investigate the effect of external factors, such as environmental noise, thermal noise, and waves on the sea surface [32]. We assume there is no

problem regarding external noises from the outside of the target area of our proposed location system because the attenuation of an undersea electromagnetic wave is considerably large. We are currently studying the effect of waves on the sea surface and have found that the wave height on the sea surface has no effect on our proposed position estimation. This will be published in the near future. Furthermore, we need to consider the antenna radiation pattern and the radiated power from a wearable transmitter on the human body. Regarding the radiation pattern, we plan to address this issue by increasing the number of polarizations with cross-dipole antennas for Rx's. This is because the electromagnetic waves received by cross-dipole antennas are omnidirectional. The effect on the radiated power difference from a wearable transmitter in the presence of the human body on our proposed system is one of the next important issues to investigate.

## ACKNOWLEDGMENT

The authors would like to thank Editage ([www.editage.com](http://www.editage.com)) for English language editing.

## REFERENCES

- [1] E. Jimenez *et al.*, "Investigation on radio wave propagation in shallow seawater: Simulations and measurements," in *Proc. IEEE 3rd Underwater Commun. Netw. Conf. (UComms)*, Aug. 2016, pp. 1–5.
- [2] D. Pompili and I. Akyildiz, "Overview of networking protocols for underwater wireless communications," *IEEE Commun. Mag.*, vol. 47, no. 1, pp. 97–102, Jan. 2009.
- [3] Marine Industry Research Group, "The research report of the development of ocean businesses and the effects of new business creation by the advanced underwater acoustic communication," Jpn. Fed. Machinery Manufacturers, Ocean Ind. Res. Group, Tokyo, Japan, Tech. Rep. JMF(Japan Machinery Federation)16, Advanced 15, 2005.
- [4] R. Otnes *et al.*, "A roadmap to ubiquitous underwater acoustic communications and networking," in *Proc. 3rd Int. Conf. Underwater Acoustic Meas. Tech. Results*, Jun. 2009, pp. 1–8.
- [5] M. Chitre, S. Shahabudeen, and M. Stojanovic, "Underwater acoustic communications and networking: Recent advances and future challenges," *Mar. Technol. Soc. J.*, vol. 42, no. 1, pp. 103–116, Mar. 2008.
- [6] T. Ohama, K. Takizawa, and T. Ikegami, "Performance evaluation on radio communications in the sea," *IEICE Tech. Rep.*, vol. 113, no. 275, pp. 65–70, Oct. 2013.
- [7] R. K. Moore, "Radio communication in the sea," *IEEE Spectr.*, vol. 4, no. 11, pp. 42–51, Nov. 1967.
- [8] M. B. Kraichman, "Basic experimental studies of the magnetic field from electromagnetic sources immersed in a semi-infinite conducting medium," *J. Res. Nat. Bur. Stand.*, vol. 64D, pp. 21–25, Jan./Feb. 1960.
- [9] R. K. Moore, "Theory of radio communication between submerged submarines," Ph.D. dissertation, Cornell Univ. Press, Ithaca, NY, USA, 1951, p. 0063.
- [10] M. Siegel and R. King, "Electromagnetic propagation between antennas submerged in the ocean," *IEEE Trans. Antennas Propag.*, vol. AP-21, no. 4, pp. 507–513, Jul. 1973.
- [11] H. Yoshida *et al.*, "Study on land-to-underwater communication," in *Proc. 14th Int. Symp. Wireless Pers. Multimedia Commun. (WPMC)*, Brest, France, 2011, pp. 1–5.
- [12] H. Sato *et al.*, "Dipole antenna with sheath-cover for seawater use," in *Proc. Int. Symp. Antennas Propag. (ISAP)*, Phuket, Thailand, Oct. 2017, pp. 1–2.
- [13] N. Ishii, Y. Ishizuka, S. Meguro, M. Takahashi, H. Yoshida, and Q. Chen, "3D measurement of transmission between small dipole antennas using pseudo scale model for underwater positioning system in KHz band," *Proc. AWPT2018, SA-3-I*, Nov. 2018, pp. 1–4.
- [14] A. I. Al-Shamma'a, A. Shaw, and S. Saman, "Propagation of electromagnetic waves at MHz frequencies through seawater," *IEEE Trans. Antennas Propag.*, vol. 52, no. 11, pp. 2843–2849, Nov. 2004.
- [15] R. W. P. King and G. S. Smith, *Antennas in Matter: Fundamentals, theory and applications*. Cambridge, MA, USA: MIT Press, 1981.

- [16] K. Shizuno, S. Yoshida, M. Tanomura, and Y. Hama, "Long distance high efficient underwater wireless charging system using dielectric-assist antenna," in *Proc. Oceans St. John's*, Sep. 2014, pp. 1–3.
- [17] A. Shaw, A. I. Al-Shamma'a, S. R. Wylie, and D. Toal, "Experimental investigations of electromagnetic wave propagation in seawater," in *Proc. Eur. Microw. Conf.*, Sep. 2006, pp. 572–575.
- [18] M. R. Frater, M. J. Ryan, and R. M. Dunbar, "Electromagnetic communications within swarms of autonomous underwater vehicles," in *Proc. WUWNet*, Sep. 2006, pp. 64–70.
- [19] X. Che, I. Wells, G. Dickers, P. Kear, and X. Gong, "Re-evaluation of RF electromagnetic communication in underwater sensor networks," *IEEE Commun. Mag.*, vol. 48, no. 12, pp. 143–151, Dec. 2010.
- [20] Regional Division Community Safety Bureau National Police Agency. *The Overview of Water Accidents in 2018*. Accessed: Jun. 2019. [Online]. Available: [https://www.npa.go.jp/publications/statistics/safetylife/chiiki/300621mi-zu\\_nennpou.pdf](https://www.npa.go.jp/publications/statistics/safetylife/chiiki/300621mi-zu_nennpou.pdf)
- [21] D. Hiyoshi and M. Takahashi, "Localization method using received signal strength for wireless power transmission of capsule endoscope," in *Proc. Int. Symp. Antennas Propag. (ISAP)*, Oct. 2017, pp. 1–2.
- [22] R. Kato, M. Takahashi, N. Ishii, Q. Chen, and H. Yoshida, "Investigation of a 3D undersea positioning system using electromagnetic waves," in *Proc. 23rd Int. Conf. Appl. Electromagn. Commun. (ICECOM)*, Sep. 2019, pp. 1–3.
- [23] A. Hales *et al.*, "The effect of salinity and temperature on electromagnetic wave attenuation in brine," *Int. J. Refrig.*, vol. 51, pp. 161–168, Mar. 2015.
- [24] Q. Chen, M. Takahashi, and N. Ishii, "Exploring EM wave applications under sea water—Concept of positioning system using amplitude decay," IEICE, Tokyo, Japan, Tech. Rep. AP2016-92, Sep. 2016, pp. 25–28.
- [25] R. W. P. King and M. F. Brown, "Lateral electromagnetic waves along plane boundaries: A summarizing approach," *Proc. IEEE*, vol. 72, no. 5, pp. 595–611, May 1984.
- [26] R. W. P. King, M. Owens, and T. T. Wu, *Lateral Electromagnetic Waves*. Springer-Verlag, 1992.
- [27] U. M. Cella, R. Johnstone, and N. Shuley, "Electromagnetic wave wireless communication in shallow water coastal environment: Theoretical analysis and experimental results," in *Proc. 4th ACM Int. Workshop UnderWater Netw. (WUWNet)*, vol. 3, Nov. 2009, pp. 1–8.
- [28] A. Emelyanenko, S. G. O'Keefe, H. G. Espinosa, and D. V. Thiel, "Surface field measurements from a buried UHF transmitter: Theory, modeling and experimental results," *IEEE Trans. Antennas Propag.*, vol. 65, no. 8, pp. 4389–4393, Aug. 2017.
- [29] Y. A. Salchak, H. G. Espinosa, and D. V. Thiel, "Modeling the surface field from an ingested radio transmitter with an approximate attenuation model for gastroenterology investigations," *IEEE Trans. Biomed. Eng.*, vol. 67, no. 2, pp. 504–511, Feb. 2020.
- [30] H. Yoshida *et al.*, "Underwater LF wave propagation study for positioning," in *Proc. OCEANS Aberdeen*, Jun. 2017, pp. 1–5.
- [31] M. Siegel and R. King, "Radiation from linear antennas in a dissipative half-space," *IEEE Trans. Antennas Propag.*, vol. AP-19, no. 4, pp. 477–485, Jul. 1971.
- [32] J. R. Wait, "The electromagnetic fields of a horizontal dipole in the presence of a conducting half-space," *Can. J. Phys.*, vol. 39, no. 7, pp. 1017–1028, Jul. 1961.
- [33] R. E. Collin, *Antennas and Radiowave Propagation*. New York, NY, USA: McGraw-Hill, 1985.



**Ryosuke Kato** (Member, IEEE) was born in Chiba, Japan, on October 2, 1994. He received the B.E. degree from Chiba University, Chiba, Japan, in 2019, where he is currently pursuing the M.E. degree, with a focus on the research on Antenna engineering.



**Masaharu Takahashi** (Senior Member, IEEE) was born in Chiba, Japan, in December, 1965. He received the B.E. degree in electrical engineering from Tohoku university, Miyagi, Japan, in 1989, and the M.E. and D.E. degrees in electrical engineering from the Tokyo Institute of Technology, Tokyo, Japan, in 1991 and 1994, respectively.

From 1994 to 1996, he was a Research Associate, and from 1996 to 2000, he was an Assistant Professor with the Musashi Institute of Technology, Tokyo. From 2000 to 2004, he was an Associate Professor with the Tokyo University of Agriculture and Technology, Tokyo. He is currently an Associate Professor with the Research Center for Frontier Medical Engineering, Chiba University, Chiba, Japan. His main interests are electrically small antennas, planar antennas, and EM compatibility.

Dr. Takahashi was the recipient of the 1994 IEEE Antennas and Propagation Society (IEEE AP-S) Tokyo Chapter Young Engineer Award.



**Nozomu Ishii** (Member, IEEE) was born in Sapporo, Japan, on October, 1966. He received the B.E., M.S., and Ph.D. degrees from Hokkaido University, Hokkaido, Japan, in 1989, 1991, and 1996, respectively.

In 1991, he joined the Faculty of Engineering of Hokkaido University. Since 1998, he has been with the Faculty of Engineering of Niigata University, Japan, where he is currently an Associate Professor of the Smart Information System Program. His current research interests are in the areas of small antennas and antenna measurements.

Dr. Ishii is a Senior Member of the Institute of Electronics, Information and Communication Engineers (IEICE). He served as General Chair for 2017 IEEE CAMA in 2017. He received the Young Engineers Award from the IEICE of Japan in 1995. He received the 2015 Best Paper Award from the IEICE Communication Society, and the 2018 IEEE Ulrich L. Rohde Innovative Conference Paper Award at the IEEE Conference on Antenna Measurements and Applications (IEEE CAMA), Västerås, Sweden.



**Qiang Chen** (Senior Member, IEEE) received the B.E. degree from Xidian University, Xi'an, China, in 1986, and the M.E. and D.E. degrees from Tohoku University, Sendai, Japan, in 1991 and 1994, respectively.

He is currently a Chair Professor of the Electromagnetic Engineering Laboratory, Department of Communications Engineering, Faculty of Engineering, Tohoku University. His primary research interests include antennas, microwave and millimeter wave, electromagnetic measurement and computational electromagnetics.

Dr. Chen is a fellow of IEICE. He received the Best Paper Award and Zen-ichi Kiyasu Award in 2009 from the Institute of Electronics, Information and Communication Engineers (IEICE). He served as the Chair for IEICE Technical Committee on Photonics-applied Electromagnetic Measurement from 2012 to 2014, the IEICE Technical Committee on Wireless Power Transfer from 2016 to 2018, the IEEE Antennas and Propagation Society Tokyo Chapter from 2017 to 2018. He is currently the Chair of IEICE Technical Committee on Antennas and Propagation.



**Hiroshi Yoshida** (Member, IEEE) received the B.S. degree in physics from the Tokyo University of Science, Tokyo, Japan, and the M.S. and Dr.Sci. degrees in physics from Kanazawa University, Japan.

He has been studying underwater vehicle technologies for the past 15 years and has led efforts to apply the technology for a variety of applications. He is currently the Deputy Director of the Engineering Department, JAMSTEC, Yokosuka, Japan. His current interests include research and development of underwater robots as well as underwater electromagnetics.